New equations for phase evaluation in measurements with an arbitrary but constant phase shift between captured intensity signs

Pedro Americo Almeida Magalhães, Jr.
Perrin Smith Neto
Cristina Almeida Magalhães
Pontificia Universidade Catolica de Minas Gerais
Av. Dom Jose Gaspar 500
Belo Horizonte, Minas Gerais 30535-610
Brasil
E-mail: paamj@oi.com.br

Clovis Sperb de Barcellos
Universidade Federal de Santa Catarina
Campus Universitário Reitor João David Ferreira Lima
Bairro Trindade, Florianópolis
Santa Catarina, CEP 88.040-900
Brasil

Abstract. We offer new equations for phase evaluation in measurements. Several phase-shifting equations with an arbitrary but constant phase shift between captured intensity signs are proposed. We show a mathematical model that seeks new equations by minimizing the uncertainty in measurements. The equations are similarly derived as the so-called Carré equation. The idea is to develop a generalization of the Carré equation that is not restricted to four images. Errors and random noise in the images cannot be eliminated, but the uncertainty due to their effects can be reduced by increasing the number of observations. An experimental analysis of the mistakes of the technique was made, as well as a detailed analysis of mistakes of the measurement. The advantages of the proposed equation are its precision in the measures taken, speed of processing, and the immunity to noise in signs and images.
 [DOI: 10.1117/1.3265438]

Subject terms: metrology; moiré techniques; fringe analysis; phase measurement; phase shifting technique; Carré equation.

Paper 090054R received Jan. 24, 2009; revised manuscript received Aug. 31, 2009; accepted for publication Sep. 23, 2009; published online Nov. 25, 2009.

1 Introduction

Conventional phase-shifting equations require phase-shift amounts to be known; however, errors on phase-shifts are common for the phase-shift modulators in real applications, and such errors can further cause substantial errors in the determination of phase distributions.[1–3] There are many potential error sources, which may affect the accuracy of the practical measurement (e.g., the phase shifting errors, detector nonlinearities, quantization errors, source stability, vibrations and air turbulence, and so on).[4]

Currently, the phase-shifting technique is the most widely used technique for evaluation of interference fields in many areas of science and engineering. Its principle is based on the evaluation of the phase values from several phase-modulated measurements of the intensity of the interference field. The phase-shifting technique offers fully automatic calculation of the phase difference between two coherent wave fields that interfere in the process.[5]

2 Theory of Phase Shifting Technique

The fringe pattern is assumed to be a sinusoidal function and is represented by intensity distribution $I(x,y)$. This function can be written in general form as

$$I(x,y) = I_m(x,y) + I_a(x,y)\cos[\phi(x,y) + \delta], \quad (1)$$

where I_m is the background intensity variation, I_a is the modulation strength, $\phi(x,y)$ is the phase at origin, and δ is the phase shift related to the origin.[6]

The general theory of synchronous detection can be applied to the discrete sampling procedure, with only a few sample points. There must be at least four signal measurements needed to determine the phase ϕ and the term δ. Phase shifting is the preferred technique whenever the external turbulence and mechanical conditions of the images remain constant over the time required to obtain the four phase-shifted frames. Typically, the technique used in this experiment is called the Carré equation.[7] By solving Eq. (1), the phase ϕ can be determined. The intensity distribution of the fringe pattern in a pixel may be represented by gray level, which varies from 0 to 255. With the Carré equation, the phase shift (δ) amount is treated as an unknown value. The equation uses four phase-shifted images as

$$\begin{cases} I_1(x,y) = I_m(x,y) + I_a(x,y)\cos\left[\phi(x,y) - \dfrac{3\delta}{2}\right] \\ I_2(x,y) = I_m(x,y) + I_a(x,y)\cos\left[\phi(x,y) - \dfrac{\delta}{2}\right] \\ I_3(x,y) = I_m(x,y) + I_a(x,y)\cos\left[\phi(x,y) + \dfrac{\delta}{2}\right] \\ I_4(x,y) = I_m(x,y) + I_a(x,y)\cos\left[\phi(x,y) + \dfrac{3\delta}{2}\right] \end{cases}. \quad (2)$$

0091-3286/2009/$25.00 © 2009 SPIE

Assuming the phase shift is linear and does not change during the measurements, the phase at each point is determined as

$$\phi = \arctan\left\{\frac{([(I_1 - I_4) + (I_2 - I_3)][3(I_2 - I_3) - (I_1 - I_4)])^{1/2}}{(I_2 + I_3) - (I_1 + I_4)}\right\}. \tag{3}$$

Expanding Eq. (3), we obtain the Carré equation as

$$\tan(\phi) = \frac{\left(\left|\begin{matrix} -I_1^2 & +2I_1I_2 & -2I_1I_3 & +2I_1I_4 \\ & +3I_2^2 & -6I_2I_3 & -2I_2I_4 \\ & & +3I_3^2 & +2I_3I_4 \\ & & & -I_4^2 \end{matrix}\right|\right)^{1/2}}{|-I_1 + I_2 + I_3 - I_4|} \tag{4}$$

or emphasizing only the matrix of coefficients of the numerator and denominator,

$$\tan(\phi) = \frac{\left(\left|\sum_{r=1}^{4}\sum_{s=r}^{4} n_{r,s}I_rI_s\right|\right)^{1/2}}{\left|\sum_{r=1}^{4} d_rI_r\right|} \begin{cases} \text{Num} = \begin{bmatrix} n_{1,1} & n_{1,2} & n_{1,3} & n_{1,4} \\ & n_{2,2} & n_{2,3} & n_{2,4} \\ & & n_{3,3} & n_{3,4} \\ & & & n_{4,4} \end{bmatrix}, & \text{Dem} = [d_1\ d_2\ d_3\ d_4] \\ \text{Num} = \begin{bmatrix} -1 & 2 & -2 & 2 \\ & 3 & -6 & -2 \\ & & 3 & 2 \\ & & & -1 \end{bmatrix}, & \text{Dem} = [-1\ 1\ 1\ -1]. \end{cases} \tag{5}$$

Almost all the existing phase-shifting equations are based on the assumption that the phase-shift at all pixels of the intensity frame is equal and known. However, it may be very difficult to achieve this in practice. Phase-measuring equations are more or less sensitive to some types of errors that can occur during measurements with images. The phase-shift value is assumed unknown but constant in phase calculation equations, which are derived in this paper. Consider now the constant but unknown phase-shift value δ between recorded images of the intensity of the observed interference field.

Considering N phase-shifted intensity measurements, we can write for the intensity distribution I_k at every point of k recorded phase-shifted interference patterns.

$$I_k(x,y) = I_m(x,y) + I_a(x,y)\cos\left[\phi(x,y) + \left(\frac{2k - N - 1}{2}\right)\delta\right], \tag{6}$$

where $k = 1, \ldots, N$ and N being the number of frames.

In Novak,[4] several five-step phase-shifting equations insensitive to phase-shift calibration are described and a complex error analysis of these phase calculation equations is performed. The best five-step equation [Eq. (7)] seems to be a very accurate and stable phase-shifting equation with the unknown phase step for a wide range of phase-step values.

$$\begin{cases} a_{jk} = I_j - I_k \\ b_{jk} = I_j + I_k \end{cases} \quad \tan(\phi) = \frac{(4a_{24}^2 - a_{15}^2)^{1/2}}{2I_3 - b_{15}} = \frac{(4(I_2 - I_4)^2 - (I_1 - I_5)^2)^{1/2}}{2I_3 - I_1 - I_5}. \tag{7}$$

Expanding Eq. (7), we obtain the Novak equation as

$$\tan(\phi) = \frac{\left(\left|\begin{matrix} -I_1^2 & & & +2I_1I_5 \\ & +4I_2^2 & -8I_2I_4 & \\ & & +4I_4^2 & \\ & & & -I_5^2 \end{matrix}\right|\right)^{1/2}}{|-I_1 + 2I_3 - I_5|} \tag{8}$$

or emphasizing only the matrix of coefficients of the numerator and the denominator:

$$\tan(\phi)=\frac{\left(\left|\sum_{r=1}^{5}\sum_{s=r}^{5}n_{r,s}I_rI_s\right|\right)^{1/2}}{\left|\sum_{r=1}^{5}d_rI_r\right|}\begin{cases}\text{Num}=\begin{bmatrix}n_{1,1} & n_{1,2} & n_{1,3} & n_{1,4} & n_{1,5}\\ & n_{2,2} & n_{2,3} & n_{2,4} & n_{2,5}\\ & & n_{3,3} & n_{3,4} & n_{3,5}\\ & & & n_{4,4} & n_{4,5}\\ & & & & n_{5,5}\end{bmatrix}, & \text{Dem}=[d_1\ d_2\ d_3\ d_4\ d_5]\\ \text{Num}=\begin{bmatrix}-1 & 0 & 0 & 0 & 2\\ & 4 & 0 & -8 & 0\\ & & 0 & 0 & 0\\ & & & 4 & 0\\ & & & & -1\end{bmatrix}, & \text{Dem}=[-1\ 0\ 2\ 0\ -1].\end{cases} \tag{9}$$

3 Uncertainty Analysis

Following the model of uncertainty analysis presented in Ref. 8, these new equations have excellent results with the application of the Monte Carlo–based technique of uncertainty propagation. The Monte Carlo–based technique requires assigning probability density functions (PDFs) to each input quantity. A computer algorithm is set up to generate an input vector $\boldsymbol{P}=(p_1\ldots p_m)^{\mathrm{T}}$; each element p_j of this vector is generated according to the specific PDF assigned to the corresponding quantity p_j. By applying the generated vector $\boldsymbol{P}$ to the model $Q=M(P)$, the corresponding output value Q can be computed. If the simulating process is repeated m times ($m\gg 1$), the outcome is a series of indications $(q_1\ldots q_m)$, whose frequency distribution allows us to identify the PDF of Q. Then, irrespective of the form of this PDF, the estimate q_e and its associated standard uncertainty $u(q_e)$ can be calculated by

$$q_e=\frac{1}{m}\sum_{l=1}^{m}q_l \tag{10}$$

and

$$u(q_e)=\left(\frac{1}{(m-1)}\sum_{l=1}^{m}(q_l-q_e)^2\right)^{1/2}. \tag{11}$$

The influence of the error sources affecting the phase values is considered in these models through the values of the intensity I_k. This is done by modifying Eq. (6),

$$I_k(x,y)=I_m(x,y)+I_a(x,y)\cos\left[\phi(x,y)+\left(\frac{2k-N-1}{2}\right)(\delta+\theta)+\varepsilon_k\right]+\xi_k. \tag{12}$$

Comparing Eqs. (6) and (12), it can be observed that three input quantities $(\theta,\varepsilon_k,\xi_k)$ were included. θ allows us to consider, in the uncertainty propagation, the systematic error used to induce the phase shift is not adequately calibrated. The error bound allowed us to assign to θ a rectangular PDF over the interval $[-\pi/10\ \text{rad},+\pi/10\ \text{rad}]$. ε_k allows us to account for the influence of environmental perturbations. The error bound allowed us to assign to ε_k a rectangular PDF over the interval $[-\pi/20\ \text{rad},+\pi/20\ \text{rad}]$.$\xi_k$ allows us to account for the nearly random effect of the optical noise.[8] The rectangular PDFs assigned to ξ_k should be in the interval $[-10,+10]$.

The values of ϕ were considered given in the range $[0,\pi/2]$ A computer algorithm was set up to generate single values of $(\theta,\varepsilon_k,\xi_k)$ according to the corresponding PDFs. With the generated values of the input quantities, we evaluated the phase ϕ' by using the new equations. Because this simulating process and the corresponding phase evaluation were repeated $m=10^4=10{,}000$ times, we were able to form the series $(\phi'_1\ldots\phi'_{10,000})$ with the outcomes.[8]

4 Proposed Equations

Here we proposed a general equation for calculating the phase for any number, N, of images, where

$$\tan(\phi)=\frac{\left(\left|\sum_{r=1}^{N}\sum_{s=r}^{N}n_{r,s}I_rI_s\right|\right)^{1/2}}{\left|\sum_{r=1}^{N}d_rI_r\right|}, \tag{13}$$

where N is number of images, $n_{r,s}$ are coefficients of the numerator, d_r are coefficients of the denominator, r and s are index of the sum. Or, expanding the summations and allowing an arbitrary number of lines

$$\tan(\phi) = \frac{\left(\left| \begin{array}{ccccccc} n_{1,1}I_1^2 & +n_{1,2}I_1I_2 & +n_{1,3}I_1I_3 & +n_{1,4}I_1I_4 & \ldots & +n_{1,N}I_1I_N \\ & +n_{2,2}I_2^2 & +n_{2,3}I_2I_3 & +n_{2,4}I_2I_4 & \ldots & +n_{2,N}I_2I_N \\ & & +n_{3,3}I_3^2 & +n_{3,4}I_3I_4 & \ldots & +n_{3,N}I_3I_N \\ & & & +n_{4,4}I_4^2 & \ldots & +n_{4,N}I_4I_N \\ & & & & \ldots & \ldots \\ & & & & & +n_{N,N}I_N^2 \end{array} \right| \right)^{1/2}}{\left| d_1I_1 + d_2I_2 + d_3I_3 + d_4I_4 + \ldots + d_{N-1}I_{N-1} + d_NI_N \right|}. \tag{14}$$

Or, emphasizing only the matrix of coefficients of the numerator and the denominator,

$$\tan(\phi) = \frac{\left(\left| \sum_{r=1}^{N} \sum_{s=r}^{N} n_{r,s}I_rI_s \right| \right)^{1/2}}{\left| \sum_{r=1}^{N} d_rI_r \right|} \begin{cases} \text{Num} = \begin{bmatrix} n_{1,1} & n_{1,2} & n_{1,3} & n_{1,4} & \ldots & n_{1,N} \\ & n_{2,2} & n_{2,3} & n_{2,4} & \ldots & n_{2,N} \\ & & n_{3,3} & n_{3,4} & \ldots & n_{3,N} \\ & & & n_{4,4} & \ldots & n_{4,N} \\ & & & & \ldots & \ldots \\ & & & & & n_{N,N} \end{bmatrix} \\ \text{Dem} = [d_1\ d_2\ d_3\ d_4\ \ldots\ d_{N-1}\ d_N] \end{cases}. \tag{15}$$

The display of the phase calculation equation in this way permits the viewing of symmetries and plans of sparse matrix. The use of the absolute value in the numerator and denominator restricts the angle between 0 and $\pi/2$ radian but avoids negative roots, and also eliminates false angles to be found. Subsequent considerations will later remove this restriction.[4–6]

In the tested practical applications, an increase of 20% in the processing time was noted when using 16 images instead of four while processing the standard Carré equation, due to many zero coefficients. But if one changes the coefficients from integer type to real numbers, the processing time for the evaluation of phase practically doubles because real numbers use more memory and more processing time to evaluate floating point additions and multiplications, which are many in the equations with a large quantity of images.

The shift on the problem focus of obtaining equations for calculating the phase of an analytical problem of a numerical vision is a great innovation. It breaks a paradigm that was hitherto used by several authors. After several attempts in numerical modeling of the problem, the following mathematical problem was identified (16)–(19):

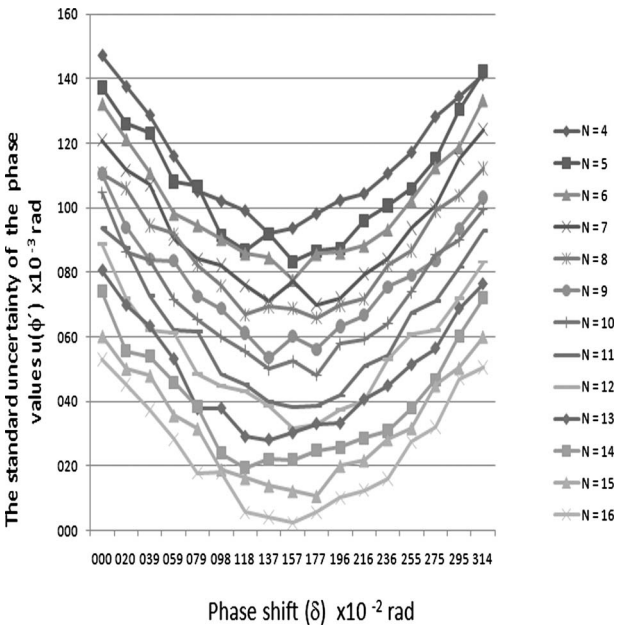

Fig. 1 Standard uncertainty of the phase values $u(\phi')$ using new equations with variation of phase shift (δ). Note that the uncertainty is smaller near $\delta = \pi/2$ radian and decreases with an increasing number of images.

$$\text{Minimal} \quad \left(\frac{\sum_{\tau=1}^{m} (\phi_*^\tau - \overline{\phi_*})^2}{m-1} \right)^{1/2} \qquad N = \text{number of images}$$

$$\text{where} \begin{cases} \overline{\phi_*} = \dfrac{\left(\sum_{\tau=1}^{m} \phi_*^\tau \right)}{m} & \text{and } m = 10000 \\ \phi_*^\tau = \arctan \left(\dfrac{\left(\left| \sum_{r=1}^{N} \sum_{s=r}^{N} n_{r,s} \hat{I}_r^\tau \hat{I}_s^\tau \right| \right)^{1/2}}{\left| \sum_{r=1}^{N} d_r \hat{I}_r^\tau \right|} \right) & \tau = 1 \ldots n \end{cases} \tag{16}$$

for each τ

$$\begin{cases} \hat{I}_k^\tau(x,y) = \hat{I}_m^\tau(x,y) + \hat{I}_a^\tau(x,y)\cos\left[\hat{\phi}^\tau(x,y) + \left(\dfrac{2k-N-1}{2} \right)(\hat{\delta}^\tau + \hat{\theta}^\tau) + \hat{\varepsilon}_k^\tau \right] + \hat{\xi}_k^\tau \text{com} & k = 1 \ldots N \\ \hat{I}_m^\tau \in [0;128] & \text{random and real} \\ \hat{I}_a^\tau \in [0;127] & \text{random and real} \\ \hat{\phi}^\tau \in \left[0; \dfrac{\pi}{2} \right] & \text{random and real} \\ \hat{\delta}^\tau \in [-2\pi; 2\pi] & \text{random and real} \\ \hat{\theta}^\tau \in \left[-\dfrac{\pi}{20}; \dfrac{\pi}{20} \right] & \text{random and real} \\ \hat{\varepsilon}_k^\tau \in \left[-\dfrac{\pi}{10}; \dfrac{\pi}{10} \right] & \text{random and real} \\ \hat{\xi}_k^\tau \in [-10; 10] & \text{ranom and real} \end{cases} \tag{17}$$

$$\text{Subject (Restriction)} \begin{cases} & \text{Variables are } n_{r,s} \text{ and } d_r & \text{Number of variables } (v) \\ (i) & \tan^2(\phi^v)\left(\sum_{r=1}^{N} d_r I_r^v \right)^2 = \sum_{r=1}^{N} \sum_{s=r}^{N} n_{r,s} I_r^v I_s^v, & v = 1 \ldots \left[\dfrac{(N+1)N}{2} + N \right] \\ (ii) & \sum_{s=r}^{N} |n_{r,s}| + |d_r| \geq 1, & r = 1 \ldots N, \text{ enter all frames} \\ (iii) & \sum_{s=r}^{N} |n_{s,r}| + |d_r| \geq 1, & r = 1 \ldots N, \text{ enter all frames} \\ (iv) & -2N \leq n_{r,s} \leq 2N, & r = 1 \ldots N, s = r \ldots N \\ (v) & -2N \leq d_r \leq 2N, & r = 1 \ldots N \\ (vi) & n_{r,s} \text{ are integer}, & r = 1 \ldots N, s = r \ldots N \\ (vii) & d_r \text{ are integer}, & r = 1 \ldots N \end{cases} , \tag{18}$$

where for each v in (i)

$$\begin{cases} I_k^v(x,y) = I_m^v(x,y) + I_a^v(x,y)\cos\left[\phi^v(x,y) + \left(\dfrac{2k-N-1}{2}\right)\delta^v\right], & k = 1\ldots N \\ I_m^v \in [0;128] & \text{random and real} \\ I_a^v \in [0;127] & \text{random and real} \\ \phi^v \in [-\pi;\pi] & \text{random and real} \\ \delta^v \in [-2\pi;2\pi] & \text{random and real} \end{cases} . \tag{19}$$

The coefficients of the matrices of the numerator $(n_{r,s})$ and the denominator (d_r) must be integers to increase the performance of the computer algorithm, as the values of the intensity of the images (I_k) are also integers ranging from 0 to 255. Modern computers perform integer computations (additions and multiplications) much faster than floating point ones. It should be noted that, currently, the commercial digital photographic cameras already present graphics resolution above 12 Mega pixels and that the evaluation of phase (ϕ) should be done pixel to pixel. Another motivation is the use of memory: integer values can be stored on a single byte while real values use, at least, 4 bytes. The present scheme uses real numbers only in the square root of the numerator, in the division by denominator and in the arc-tangent over the entire operation.

The idea is to obtain the values of the coefficients of matrices of the numerator $(n_{r,s})$ and denominator (d_r) with the minimum standard uncertainty the phase values $u(\phi')$ in Eq. (11). It comes from the attempt to force these factors to zero, for computational speed up and for reducing the required memory, because zero terms in sparse matrices do not need to be stored. It is also important that those ratios are not very large so that the sum of the numerator and denominator do not have a very high value to fit into an integer variable. For a precise phase evaluation, these factors will increase the values of the intensity of the image (I_k) that contains errors due to noise in the image, in its discretization in pixels and in shades of gray.

The first restriction of Eq. (19) is the Eq. (13), which is squared to form the relation that one is seeking. Note that the results obtained by solving the mathematical problem of the coefficients are in the form of matrices for the numerator $(n_{r,s})$ and the denominator (d_r), so the number of unknowns is given by ν. To ensure that one has a hyper-restricted problem, the number of restrictions must be greater than or at least equal to the number of variables. The ν restrictions of the model are obtained through random choice of values for I_m, I_a, ϕ, and δ and by using Eq. (6) to compute I_k. Tests showed that even for low numbers for other values of ν, the mathematical problem leads to only one optimal solution though it becomes more time consuming. That is, the mathematical model has been successful when it used the value of ν ranging from 1 to lower values as 4. Indeed the values of I_m, I_a, ϕ, and δ can be any real number, but to maintain compatibility with the problem images, it was decided to limit I_m to between 0 to 128 and I_a between 0 and 127 so that I_k would be between 0 and 255.

The restrictions (ii) and (iii) of the problem are based on the idea that all image luminous intensities, I_k, must be present in the equation. It increases the amounts of samples to reduce the noise of random images. This requires that all of the sampling images enter the equation for phase calculation. This is achieved by imposing that the sum of the absolute values of the coefficients of each row or column of the matrix of each of the numerator $(n_{r,s})$, plus the module at the rate corresponding to that image in the denominator (d_r), is $\geqslant 1$. Thus, the coefficients on an equation to calculate the phase for a given image I_k will not be all zeros, ensuring their participation in the equation.

Restrictions (iv) and (v) of the problem are used to accelerate the solution of this mathematical model. This limitation in the value of the coefficients of matrices of the numerator $(n_{r,s})$ and denominator (d_r) presents a significant reduction in the search universe and in the search of a solution for model optimization. The function to be minimized of the problem [Eq. (16)] is the uncertainty in Eq. (11). Equation (17) is the rewriting of Eq. (12). To accelerate, the resolution of the mathematical model can be done $n_{1,1}=-1$ and $d_1=-1$.

The following multistep equation for phase calculation uses well-known trigonometric relations and branch-and-bound algorithm[9] for pure integer nonlinear programming with the mathematic problem (16)–(19). The following Table 1 shows equations.

5 Tests of Uncertainty Analysis

The objectives are equations of phase calculation that are better, more accurate, more robust, and more stable for the random noise. The tests show that the optimum phase-shift interval with which the equation gives minimum uncertainty for the noise is in the vicinity of $\pi/2$ rads (Fig. 1).

Figure 2 show the relationship between the standard uncertainty and the phase values ϕ in the range $[-\pi,\pi]$. This relationship expresses the accuracy and stability of the proposed phase-shifting equations. Furthermore, the properties of the equations with respect to the change of parameters simulating the real nonlinearities of the phase-shifting device and detector were studied.

Figure 3 shows the average of the standard uncertainty $u(\phi')$ generated with values ϕ in the range $[0,\pi/2]$ by using new equations. It can be observed that the uncertainty by new equations diminishes as the number of images increases.

6 Symmetry and Sparse in Matrix of Coefficient

To solve the problem of increasing the processing time to obtain new equations for phase calculation with the increased number of variables for high values of N uses up important data. The equations showed symmetries in the matrix of coefficients of numerator and denominator (Fig. 4). Be $h=(N \text{ div } 2)+(N \bmod 2)$, where the value of $x \text{ div } y$ is the value of x/y rounded in the direction of zero to the nearest integer (integer division) and the mod operator returns the remainder obtained by dividing its operands [in other words, $x \bmod y = x-(x \text{ div } y)^{*}y$]. The symmetries are

$$\begin{cases} d_r = d_{N+1-r}, & r=1\ldots h \text{ and } r \neq N+1-r \\ n_{r,N+1-r} = -2n_{r,r}, & r=1\ldots h \text{ and } r \neq N+1-r \\ n_{N+1-s,N+1-r} = n_{r,s}, & r=1\ldots h; s=r\ldots h \text{ and } r \neq N+1-s \text{ and } s \neq N+1-r \\ n_{r,N+1-s} = -n_{r,s}, & r=1\ldots h; s=r\ldots h \text{ and } s > r \text{ and } s \neq N+1-s \\ n_{s,N+1-r} = -n_{r,s}, & r=1\ldots h; s=r\ldots h \text{ and } s > r \text{ and } s \neq N+1-r \end{cases} . \tag{20}$$

Thus, because the matrix for N also was

$$\text{Num} = \begin{bmatrix} n_{1,1} & n_{1,2} & n_{1,3} & \cdots & n_{1,h-1} & n_{1,h} & -n_{1,h} & -n_{1,h-1} & \cdots & -n_{1,3} & -n_{1,2} & -2n_{1,1} \\ & n_{2,2} & n_{2,3} & \cdots & n_{2,h-1} & n_{2,h} & -n_{2,h} & -n_{2,h-1} & \cdots & -n_{2,3} & -2n_{2,2} & -n_{1,2} \\ & & n_{3,3} & \cdots & n_{3,h-1} & n_{3,h} & -n_{3,h} & -n_{3,h-1} & \cdots & -2n_{3,3} & -n_{2,3} & -n_{1,3} \\ & & & \cdots & \cdots & \cdots & \cdots & \cdots & \cdots & \cdots & \cdots & \cdots \\ & & & & n_{h-1,h-1} & n_{h-1,h} & -n_{h-1,h} & -2n_{h-1,h-1} & \cdots & -n_{3,h-1} & -n_{2,h-1} & -n_{1,h-1} \\ & & & & & n_{h,h} & -2n_{h,h} & -n_{h-1,h} & \cdots & -n_{3,h} & -n_{2,h} & -n_{1,h} \\ & & & & & & n_{h,h} & n_{h-1,h} & \cdots & n_{3,h} & n_{2,h} & n_{1,h} \\ & & & & & & & n_{h-1,h-1} & \cdots & n_{3,h-1} & n_{2,h-1} & n_{1,h-1} \\ & & & & & & & & \cdots & \cdots & \cdots & \cdots \\ & & & & & & & & & n_{3,3} & n_{2,3} & n_{1,3} \\ & & & & & & & & & & n_{2,2} & n_{1,2} \\ & & & & & & & & & & & n_{1,1} \end{bmatrix}$$

$$\text{Dem} = [d_1\ d_2\ d_3\ d_4\ \ldots\ d_{h-1}\ d_h\ d_h\ d_{h-1}\ \ldots\ d_4\ d_3\ d_2\ d_1]. \tag{21}$$

also, the matrix for odd N was

$$\text{Num} = \begin{bmatrix} n_{1,1} & n_{1,2} & n_{1,3} & \cdots & n_{1,h-1} & n_{1,h} & -n_{1,h-1} & \cdots & -n_{1,3} & -n_{1,2} & -2n_{1,1} \\ & n_{2,2} & n_{2,3} & \cdots & n_{2,h-1} & n_{2,h} & -n_{2,h-1} & \cdots & -n_{2,3} & -2n_{2,2} & -n_{1,2} \\ & & n_{3,3} & \cdots & n_{3,h-1} & n_{3,h} & -n_{3,h-1} & \cdots & -2n_{3,3} & -n_{2,3} & -n_{1,3} \\ & & & \cdots & \cdots & \cdots & \cdots & \cdots & \cdots & \cdots & \cdots \\ & & & & n_{h-1,h-1} & n_{h-1,h} & -2n_{h-1,h-1} & \cdots & -n_{3,h-1} & -n_{2,h-1} & -n_{1,h-1} \\ & & & & & n_{h,h} & n_{h-1,h} & \cdots & n_{3,h} & n_{2,h} & n_{1,h} \\ & & & & & & n_{h-1,h-1} & \cdots & n_{3,h-1} & n_{2,h-1} & n_{1,h-1} \\ & & & & & & & \cdots & \cdots & \cdots & \cdots \\ & & & & & & & & n_{3,3} & n_{2,3} & n_{1,3} \\ & & & & & & & & & n_{2,2} & n_{1,2} \\ & & & & & & & & & & n_{1,1} \end{bmatrix}$$

$$\text{Dem} = [d_1\ d_2\ d_3\ d_4\ \ldots\ d_{h-1}\ d_h\ d_{h-1}\ \ldots\ d_4\ d_3\ d_2\ d_1]. \tag{22}$$

Table 1 Matrix of coefficient for $N=4,5,6,\ldots,16$.

Num	-1	2	-2	2
		3	-6	-2
N = 4			3	2
				-1
Dem	-1	1	1	-1

Num	-1	0	0	0	2
		4	0	-8	0
N = 5			0	0	0
				4	0
Dem	-1	0	2	0	-1

Num	-1	0	-1	1	0	2
		3	1	-1	-6	0
N = 6			0	0	-1	1
				0	1	-1
					3	0
						-1
Dem	-1	0	1	1	0	-1

N = 7	Num	-1	-2	-3	0	3	2	2
			4	6	0	-6	-8	2
				2	0	-4	-6	3
	N = 7				0	0	0	0
						2	6	-3
							4	-2
								-1
	Dem	-1	-1	1	2	1	-1	-1

Num	-1	0	1	0	0	-1	0	2
		1	0	-2	2	0	-2	0
			1	1	-1	-2	0	-1
				1	-2	-1	2	0
N = 8					1	1	-2	0
						1	0	1
							1	0
								-1
Dem	-1	0	1	0	0	1	0	-1

Num	-1	2	-1	1	0	-1	1	-2	2
		0	-3	1	0	-1	3	0	-2
			5	-5	0	5	-10	3	1
				1	0	-2	5	-1	-1
N = 9					0	0	0	0	0
						1	-5	1	1
							5	-3	-1
								0	2
									-1
Dem	-1	1	0	-1	2	-1	0	1	-1

Num	-1	0	1	0	0	0	0	0	-1	0	2
		1	0	-1	0	0	1	0	-2	0	0
			1	0	0	-1	1	0	0	0	-1
				1	1	-1	-2	0	1	0	
					1	-2	-1	1	0	0	
N = 10						1	1	-1	0	0	
							1	0	-1	0	
								0	0	1	
									1	0	
										-1	
Dem	-1	0	1	0	0	0	0	1	0	-1	

Num	-1	0	-1	-2	0	0	0	2	1	0	2
		1	0	0	2	0	-2	0	0	-2	0
			2	2	0	0	0	-2	-4	0	1
				1	0	0	0	-2	-2	0	2
					2	0	-4	0	0	-2	0
N = 11						0	0	0	0	0	0
							2	0	0	2	0
								1	2	0	-2
									2	0	-1
										1	0
											-1
Dem	-1	0	0	-1	1	2	1	-1	0	0	-1

Num	-1	0	1	0	0	0	0	0	0	-1	0	2
		1	0	-1	0	0	0	0	1	0	-2	0
			0	0	-1	0	0	1	0	0	0	-1
				1	0	0	0	0	-2	0	1	0
					0	1	-1	0	0	1	0	0
N = 12						1	-2	-1	0	0	0	0
							1	1	0	0	0	0
								0	0	-1	0	0
									1	0	-1	0
										0	0	1
											1	0
												-1
Dem	-1	0	1	0	0	0	0	0	0	1	0	-1

Num	-1	2	-2	-2	0	1	0	-1	0	2	2	-2	2
		1	0	0	-1	1	0	-1	1	0	0	-2	-2
N = 13			2	0	0	-1	0	1	0	0	-4	0	2
				2	-2	-1	0	1	2	-4	0	0	2
					2	-2	0	2	-4	2	0	1	0
						-1	0	2	2	1	1	-1	-1
N = 13							0	0	0	0	0	0	0
								-1	-2	-1	-1	1	1
								2	-2	0	-1	0	
									2	0	0	-2	
										2	0	-2	
											1	2	
												-1	
Dem	-1	1	0	-1	0	0	2	0	0	-1	0	1	-1

Num	-1	0	1	0	0	0	0	0	0	0	-1	0	2
		1	0	-1	0	0	0	0	0	1	0	-2	0
			0	0	1	0	0	0	0	-1	0	0	-1
				-1	0	-1	0	0	1	0	2	0	1	0
					1	0	-2	0	-1	1	0	0	0	
						1	1	-1	-2	0	1	0	0	
N = 14							1	-2	-1	1	0	0	0	
								1	1	-1	0	0	0	
									1	0	-1	0	0	
										1	0	1	0	
											-1	0	-1	
												0	0	1
													1	0
														-1
Dem	-1	0	1	0	0	0	0	0	0	0	0	1	0	-1

Num	-1	-2	-1	1	0	0	0	0	0	0	-1	1	2	2
		2	1	-2	-1	0	0	0	0	1	2	-1	-4	2
			1	1	-1	2	0	0	-2	1	-1	-2	-1	1
				1	2	2	-2	0	2	-2	-2	-2	-1	2
					2	-2	1	0	-1	2	-4	-2	1	1
						-1	0	0	0	2	2	-2	-2	0
							1	0	-2	0	-1	2	0	0
N = 15								0	0	0	0	0	0	0
									1	0	1	-2	0	0
										-1	-2	2	2	0
											2	2	-1	-1
												1	1	-2
													1	1
														2
														-1
Dem	-1	-1	1	0	0	0	0	2	0	0	0	0	1	-1

Num	-1	0	1	0	0	0	0	0	0	0	0	0	-1	0	2
		1	0	-1	0	0	0	0	0	0	0	1	0	-2	0
			0	0	1	0	0	0	0	0	-1	0	0	0	-1
				-1	0	0	0	0	0	0	0	2	0	1	0
					0	0	-1	0	0	1	0	0	0	-1	0
						1	0	-1	0	0	-2	0	0	0	0
N = 16							1	1	-1	0	0	0	0	0	0
								1	0	-1	0	0	0	0	0
									1	0	0	0	0	0	0
										0	0	1	0	0	0
											-1	0	-1	0	
												0	0	1	
													1	0	
														-1	
Dem	-1	0	1	0	0	0	0	0	0	0	0	0	1	0	-1

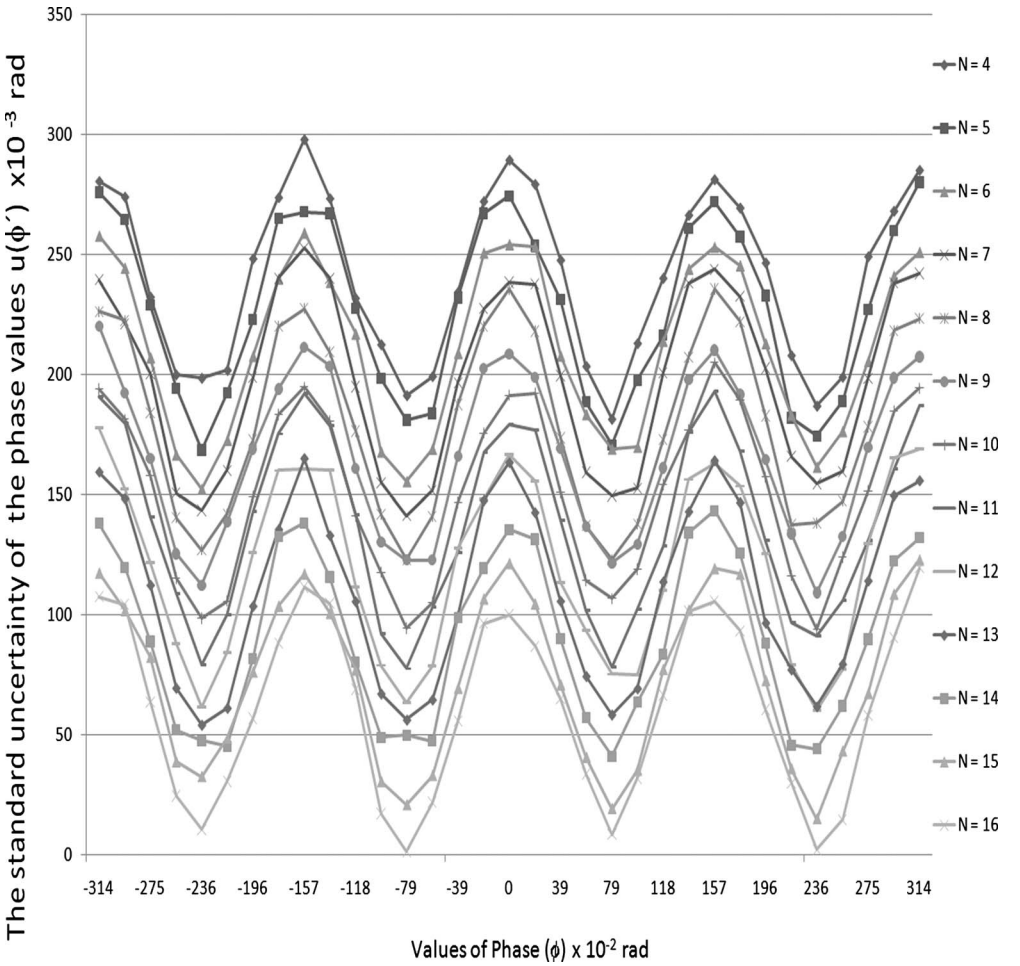

Fig. 2 Standard uncertainty of the phase values $u(\phi')$ using new equations with variation of phase (ϕ). Note that the uncertainty is smaller near of the multiples $\phi = \pi/4$ radian and decreases with an increasing number of images.

Fig. 3 Average of the standard uncertainty $u(\phi')$ by using new equations. Note that the uncertainty decreases with an increasing number of images.

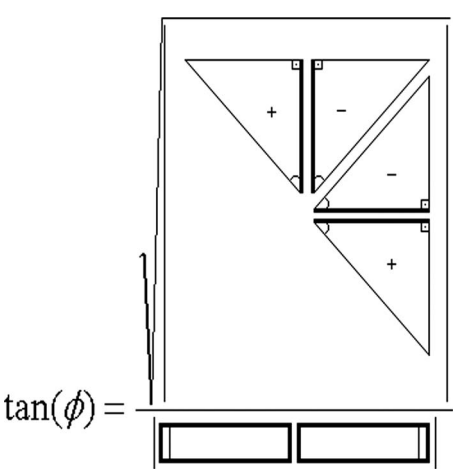

Fig. 4 Symmetries in the coefficients of numerator and the denominator.

Therefore, using symmetry to the numerator coefficients can be represented with only its first quarter and the denominator coefficients can be represented only with the first half (Fig. 4), as shown below

$$\mathrm{Num}^{1/4}=\begin{bmatrix} n_{1,1} & n_{1,2} & n_{1,3} & \cdots & n_{1,h-1} & n_{1,h} \\ & n_{2,2} & n_{2,3} & \cdots & n_{2,h-1} & n_{2,h} \\ & & n_{3,3} & \cdots & n_{3,h-1} & n_{3,h} \\ & & & \cdots & \cdots & \cdots \\ & & & & n_{h-1,h-1} & n_{h-1,h} \\ & & & & & n_{h,h} \end{bmatrix} \quad \mathrm{Dem}^{1/2}=[d_1 \quad d_2 \quad d_3 \quad \ldots \quad d_{h-1} \quad d_h]. \tag{23}$$

In previous equations, most of the coefficients of the numerator and denominator are zero. And even more for the first quarter of the coefficients of the numerator, the terms are different from zero in the main diagonal and closer to the three diagonal; thus, only the first four coefficients of each line are different from zero. In the first half of the coefficients of the denominator, only the first four and the last term are different from zero. A matrix where most of the terms are zeros is usually called sparse matrix,

$$\text{Sparse} \quad \begin{cases} d_r^{1/2}=0, & r=5\,..\,h-1 \\ n_{r,s}^{1/4}=0, & r=1\,..\,h-5, \quad s=r+4\,..\,h, \quad \text{and } s>r+3. \end{cases} \tag{24}$$

In order, the matrix is

$$\mathrm{Num}^{1/4}=\begin{bmatrix} n_{1,1} & n_{1,2} & n_{1,3} & n_{1,4} & 0 & 0 & 0 & 0 & 0 & 0 & \cdots & 0 \\ & n_{2,2} & n_{2,3} & n_{2,4} & n_{2,5} & 0 & 0 & 0 & 0 & 0 & \cdots & 0 \\ & & n_{3,3} & n_{3,4} & n_{3,5} & n_{3,6} & 0 & 0 & 0 & 0 & \cdots & 0 \\ & & & n_{4,4} & n_{4,5} & n_{4,6} & n_{4,7} & 0 & 0 & 0 & \cdots & 0 \\ & & & & \cdots & \cdots & \cdots & \cdots & 0 & 0 & \cdots & 0 \\ & & & & & n_{h-6,h-6} & n_{h-6,h-5} & n_{h-6,h-4} & n_{h-6,h-3} & 0 & \cdots & 0 \\ & & & & & & n_{h-5,h-5} & n_{h-5,h-4} & n_{h-5,h-3} & n_{h-5,h-2} & 0 & 0 \\ & & & & & & & n_{h-4,h-4} & n_{h-4,h-3} & n_{h-4,h-2} & n_{h-4,h-1} & 0 \\ & & & & & & & & n_{h-3,h-3} & n_{h-3,h-2} & n_{h-3,h-1} & n_{h-3,h} \\ & & & & & & & & & n_{h-2,h-2} & n_{h-2,h-1} & n_{h-2,h} \\ & & & & & & & & & & n_{h-1,h-1} & n_{h-1,h} \\ & & & & & & & & & & & n_{h,h} \end{bmatrix}$$

$$\mathrm{Dem}^{1/2}=[d_1 \quad d_2 \quad d_3 \quad d_4 \quad 0 \quad 0 \quad \ldots \quad 0 \quad 0 \quad d_h]. \tag{25}$$

An important fact is that the resolution of the mathematical model generates new and efficient equations for calculating the phase. Because most of the coefficients of both the numerator and denominator is zero, the implementation of these new equations is very fast and the volume of mathematical operations is reduced because the terms are zero as there is no need for multiplier to the values of luminous intensity I_k for these factors, because any number multiplied by zero will be zero.

7 Equations for Phase Calculation of Many Images

Analyzing the equations deducted, we attempted to get a rule for generation or an algorithm to provide valid values of coefficients of the numerator and the denominator of the equations for phase calculation of large quantities of images ($N > 15$). The concept of symmetry and sparse matrix of the previous section was used to look for a rule of training for the first four terms of each line of the fourth coefficient of the numerator, and for the four words, which may be different from zero to half the denominator. The first thing that was done was to reset all the coefficients of the numerator and denominator.

The rule that established training is divided into eight cases, depending on the value of the number of images (N). For each case, there was training with a rule shown below.

For case 1, when N is even, N is divisible by 4 and N is also divisible by 8

$$\text{Half} = N/2$$
$$\text{Fourth} = N/4$$

$$\text{Num}^{1/4} = \begin{bmatrix}
-1 & 0 & 1 & 0 & \dots & & & & & & & & & & \text{Row:} \\
 & 1 & 0 & -1 & 0 & \dots & & & & & & & & & 1 \\
 & & & 0 & 0 & 1 & 0 & \dots & & & & & & & 2 \\
 & & & & -1 & 0 & 0 & 0 & \dots & & & & & & 3 \\
 & & & & & 0 & 0 & 1 & 0 & \dots & & & & & 4 \\
 & & & & & & -1 & 0 & 0 & 0 & \dots & & & & \text{Repeat} \\
 & & & & & & & \dots & \dots & \dots & \dots & \dots & & & \text{Repeat} \\
 & & & & & & & & 0 & 0 & -1 & 0 & \dots & & \dots \\
 & & & & & & & & & 1 & 0 & 0 & 0 & \dots & \text{Fourth}+1 \\
 & & & & & & & & & & 0 & 0 & -1 & 0 & \text{Fourth}+2 \\
 & & & & & & & & & & & 1 & 0 & 0 & \text{Repeat} \\
 & & & & & & & & & & & & \dots & \dots & \text{Repeat} \\
 & & & & & & & & & & & & 1 & 0 & \dots \\
 & & & & & & & & & & & & & 1 & \text{Half}-2 \\
 & & & & & & & & & & & & & & \text{Half}-1 \\
 & & & & & & & & & & & & & & \text{Half}
\end{bmatrix}$$

$$\text{Dem}^{1/2} = [-1 \quad 0 \quad 1 \quad 0 \quad 0 \quad 0 \quad \dots \quad 0 \quad 0 \quad 0]$$
$$\text{Col} \quad : 1 \quad 2 \quad 3 \quad 4 \quad 5 \quad 6 \quad \dots \quad \text{Half}-2 \quad \text{Half}-1 \quad \text{Half} \tag{26}$$

For case 2, when N is even, N is divisible by 4 but N is not divisible by 8

$\text{Half} = N/2$

$\text{Fourth} = N/4$

$$\text{Num}^{1/4} = \begin{bmatrix} -1 & 0 & 1 & 0 & \dots & & & & & & & & \\ & 1 & 0 & -1 & 0 & \dots & & & & & & & \\ & & & 0 & 0 & 1 & 0 & \dots & & & & & \\ & & & & -1 & 0 & 0 & 0 & \dots & & & & \\ & & & & & 0 & 0 & 1 & 0 & \dots & & & \\ & & & & & & -1 & 0 & 0 & 0 & \dots & & \\ & & & & & & & \dots & \dots & \dots & \dots & \dots & \\ & & & & & & & & 0 & 0 & -1 & 0 & \dots \\ & & & & & & & & & 1 & 0 & 0 & 0 \\ & & & & & & & & & & 0 & 0 & -1 \\ & & & & & & & & & & & 1 & 0 \\ & & & & & & & & & & & & \dots \\ & & & & & & & & & & & 0 & 1 \\ & & & & & & & & & & & & 1 \end{bmatrix} \begin{matrix} \text{Row:} \\ 1 \\ 2 \\ 3 \\ 4 \\ \text{Repeat} \\ \text{Repeat} \\ \dots \\ \text{Fourth} \\ \text{Fourth} + 1 \\ \text{Repeat} \\ \text{Repeat} \\ \dots \\ \\ \text{Half} - 1 \\ \text{Half} \end{matrix}$$

$$\begin{matrix} \text{Dem}^{1/2} = [-1 & 0 & 1 & 0 & 0 & 0 & \dots & 0 & 0 & 0] \\ \text{Col} \quad :1 & 2 & 3 & 4 & 5 & 6 & \dots & \text{Half} - 2 & \text{Half} - 1 & \text{Half} \end{matrix} . \tag{27}$$

For case 3, when N is even, $N+2$ is divisible by 4, and $N+2$ is divisible by 8:

$\text{Half} = N/2$

$\text{Fourth} = (N+2)/4$

$$\text{Num}^{1/4} = \begin{bmatrix} -1 & 0 & 1 & 0 & \dots & & & & & & & & & \\ & 1 & 0 & -1 & 0 & \dots & & & & & & & & \\ & & & 0 & 0 & 1 & 0 & \dots & & & & & & \\ & & & & -1 & 0 & 0 & 0 & \dots & & & & & \\ & & & & & 0 & 0 & 1 & 0 & \dots & & & & \\ & & & & & & -1 & 0 & 0 & 0 & \dots & & & \\ & & & & & & & \dots & \dots & \dots & \dots & \dots & & \\ & & & & & & & & 0 & 0 & -1 & 0 & \dots & \\ & & & & & & & & & 1 & 0 & 0 & 0 & \\ & & & & & & & & & & 0 & 0 & -1 & \\ & & & & & & & & & & & 1 & 0 & \\ & & & & & & & & & & & & \dots & \\ & & & & & & & & & & & & 1 & 0 \\ & & & & & & & & & & & & 0 & 1 \\ & & & & & & & & & & & & & 1 \end{bmatrix} \begin{matrix} \text{Row:} \\ 1 \\ 2 \\ 3 \\ 4 \\ \text{Repeat} \\ \text{Repeat} \\ \dots \\ \text{Fourth} + 1 \\ \text{Fourth} + 2 \\ \text{Repeat} \\ \text{Repeat} \\ \dots \\ \text{Half} - 3 \\ \text{Half} - 2 \\ \text{Half} - 1 \\ \text{Half} \end{matrix}$$

$$\begin{matrix} \text{Dem}^{1/2} = [-1 & 0 & 1 & 0 & 0 & 0 & \dots & 0 & 0 & 0] \\ \text{Col} \quad :1 & 2 & 3 & 4 & 5 & 6 & \dots & \text{Half} - 2 & \text{Half} - 1 & \text{Half} \end{matrix} . \tag{28}$$

For case 4, when N is even, $N+2$ is divisible by 4 but $N+2$ is not divisible by 8

$\text{Half} = N/2$

$\text{Fourth} = (N+2)/4$

$$\text{Num}^{1/4} = \begin{bmatrix} -1 & 0 & 1 & 0 & \dots & & & & & & & & \\ & 1 & 0 & -1 & 0 & \dots & & & & & & & \\ & & & 0 & 0 & 1 & 0 & \dots & & & & & \\ & & & & -1 & 0 & 0 & 0 & \dots & & & & \\ & & & & & 0 & 0 & 1 & 0 & \dots & & & \\ & & & & & & -1 & 0 & 0 & 0 & \dots & & \\ & & & & & & & \dots & \dots & \dots & \dots & \dots & \\ & & & & & & & & 0 & 0 & -1 & 0 & \dots \\ & & & & & & & & & 1 & 0 & 0 & 0 \\ & & & & & & & & & & 0 & 0 & -1 \\ & & & & & & & & & & & 1 & 0 \\ & & & & & & & & & & & & \dots \\ & & & & & & & & & & & & 1 \\ & & & & & & & & & & & & \\ & & & & & & & & & & & & \\ & & & & & & & & & & & & \end{bmatrix} \begin{matrix} \text{Row:} \\ 1 \\ 2 \\ 3 \\ 4 \\ \text{Repeat} \\ \text{Repeat} \\ \dots \\ \text{Fourth} \\ \text{Fourth}+1 \\ \text{Repeat} \\ \text{Repeat} \\ \dots \\ \text{Half}-3 \\ \text{Half}-2 \\ \text{Half}-1 \\ \text{Half} \end{matrix}$$

$$\begin{matrix} \text{Dem}^{1/2} = [-1 & 0 & 1 & 0 & 0 & 0 & \dots & 0 & 0 & 0] \\ \text{Col} \quad :1 & 2 & 3 & 4 & 5 & 6 & \dots & \text{Half}-2 & \text{Half}-1 & \text{Half} \end{matrix} . \tag{29}$$

For case 5, when N is odd, $N-1$ is divisible by 4 and $N-1$ is divisible by 8:

$\text{Half} = (N+1)/2$

$\text{Fourth} = (N-1)/4$

$$\text{Num}^{1/4} = \begin{bmatrix} -1 & 2 & -1 & 0 & \dots & & & & & & & & \\ & 0 & -2 & 0 & 0 & \dots & & & & & & & \\ & & & 2 & 0 & -1 & 0 & \dots & & & & & \\ & & & & 0 & 0 & 0 & 1 & \dots & & & & \\ & & & & & 0 & -1 & 0 & 0 & \dots & & & \\ & & & & & & \dots & \dots & \dots & \dots & \dots & & \\ & & & & & & & 0 & 0 & 2 & -2 & . & \\ & & & & & & & & 2 & -2 & 0 & 2 & \dots \\ & & & & & & & & & 0 & 2 & 0 & 0 \\ & & & & & & & & & & 0 & 0 & 0 \\ & & & & & & & & & & & 0 & 1 \\ & & & & & & & & & & & & \dots \\ & & & & & & & & & & & & \dots \\ & & & & & & & & & & & & 0 \\ & & & & & & & & & & & & \\ & & & & & & & & & & & & \end{bmatrix} \begin{matrix} \text{Row:} \\ 1 \\ 2 \\ 3 \\ \text{Repeat} \\ \text{Repeat} \\ \dots \\ \text{Fourth} \\ \text{Fourth}+1 \\ \text{Fourth}+2 \\ \text{Repeat} \\ \text{Repeat} \\ \dots \\ \dots \\ \text{Half}-2 \\ \text{Half}-1 \\ \text{Half} \end{matrix}$$

$$\begin{matrix} \text{Dem}^{1/2} = [-1 & 1 & 0 & -1 & 0 & 0 & \dots & 0 & 0 & 2] \\ \text{Col} \quad :1 & 2 & 3 & 4 & 5 & 6 & \dots & \text{Half}-2 & \text{Half}-1 & \text{Half} \end{matrix} . \tag{30}$$

For case 6, when N is odd, $N-1$ is divisible by 4 but $N-1$ is not divisible by 8,

$$\text{Half} = (N+1)/2$$
$$\text{Fourth} = (N-1)/4$$

$$\text{Num}^{1/4} = \begin{bmatrix} -1 & 2 & -1 & 0 & \dots & & & & & & & & \\ & 0 & -2 & 0 & 0 & \dots & & & & & & & \\ & & & 2 & 0 & -1 & 0 & \dots & & & & & \\ & & & & 0 & 0 & 0 & 0 & \dots & & & & \\ & & & & & 0 & 0 & 1 & 0 & \dots & & & \\ & & & & & & -1 & 0 & 0 & 0 & \dots & & \\ & & & & & & & \dots & \dots & \dots & \dots & . & \\ & & & & & & & & 0 & 0 & 2 & -2 & \dots \\ & & & & & & & & & 2 & -2 & 0 & 2 \\ & & & & & & & & & & 0 & 2 & 0 \\ & & & & & & & & & & & 0 & 0 \\ & & & & & & & & & & & 1 & 0 \\ & & & & & & & & & & & & \dots \\ & & & & & & & & & & & & 1 \\ & & & & & & & & & & & & \end{bmatrix} \begin{matrix} \text{Row:} \\ 1 \\ 2 \\ 3 \\ 4 \\ \text{Repeat} \\ \text{Repeat} \\ \dots \\ \text{Fourth} \\ \text{Fourth}+1 \\ \text{Fourth}+2 \\ \text{Repeat} \\ \text{Repeat} \\ \dots \\ \text{Half}-2 \\ \text{Half}-1 \\ \text{Half} \end{matrix}$$

$$\begin{matrix} \text{Dem}^{1/2} = [-1 & 1 & 0 & -1 & 0 & 0 & \dots & 0 & 0 & 2] \\ \text{Col} \quad :1 & 2 & 3 & 4 & 5 & 6 & \dots & \text{Half}-2 & \text{Half}-1 & \text{Half} \end{matrix} . \tag{31}$$

For case 7, when N is odd, $N+1$ is divisible by 4 and $N+1$ is divisible by 8,

$$\text{Half} = (N+1)/2$$
$$\text{Fourth} = (N+1)/4$$

$$\text{Num}^{1/4} = \begin{bmatrix} -1 & -2 & 0 & 1 & 0 & \dots & & & & & & & \\ & 1 & 1 & -1 & 0 & 0 & \dots & & & & & & \\ & & & 0 & 0 & 0 & 0 & \dots & & & & & \\ & & & & 0 & 0 & -1 & 0 & \dots & & & & \\ & & & & & 1 & 0 & 0 & 0 & \dots & & & \\ & & & & & & 0 & 0 & 1 & 0 & \dots & & \\ & & & & & & & -1 & 0 & 0 & 0 & \dots & \\ & & & & & & & & -1 & 0 & 2 & 0 & \dots \\ & & & & & & & & & 0 & 2 & 2 & -2 \\ & & & & & & & & & & 2 & -2 & 0 \\ & & & & & & & & & & & 0 & 0 \\ & & & & & & & & & & & 1 & 0 \\ & & & & & & & & & & & & \dots \\ & & & & & & & & & & & 0 & 1 \\ & & & & & & & & & & & & 1 \\ & & & & & & & & & & & & \end{bmatrix} \begin{matrix} \text{Row:} \\ 1 \\ 2 \\ 3 \\ 4 \\ 5 \\ \text{Repeat} \\ \text{Repeat} \\ \text{Fourth}-1 \\ \text{Fourth} \\ \text{Fourth}+1 \\ \text{Repeat} \\ \text{Repeat} \\ \dots \\ \text{Half}-2 \\ \text{Half}-1 \\ \text{Half} \end{matrix}$$

$$\begin{matrix} \text{Dem}^{1/2} = [-1 & -1 & 1 & 0 & 0 & 0 & \dots & 0 & 0 & 2] \\ \text{Col} \quad :1 & 2 & 3 & 4 & 5 & 6 & \dots & \text{Half}-2 & \text{Half}-1 & \text{Half} \end{matrix} . \tag{32}$$

For case 8, when N is odd, $N+1$ is divisible by 4 but $N+1$ is not divisible by 8

$$\text{Half} = (N+1)/2$$
$$\text{Fourth} = (N+1)/4$$

$$\text{Num}^{1/4} = \begin{bmatrix} -1 & -2 & 0 & 0 & 0 & \dots & & & & & & & & \\ & 1 & 2 & -1 & 0 & 0 & \dots & & & & & & & \\ & & & 0 & 0 & -1 & 0 & \dots & & & & & & \\ & & & & 1 & 0 & 0 & 0 & \dots & & & & & \\ & & & & & 0 & 0 & 1 & 0 & \dots & & & & \\ & & & & & & -1 & 0 & 0 & 0 & \dots & & & \\ & & & & & & & \dots & \dots & \dots & \dots & \dots & & \\ & & & & & & & & -1 & 0 & 2 & 0 & \dots & \\ & & & & & & & & & 0 & 2 & 2 & -2 & 0 & \dots \\ & & & & & & & & & & 2 & -2 & 0 & 0 & \dots \\ & & & & & & & & & & & 0 & 0 & -1 & 0 & \dots \\ & & & & & & & & & & & & 1 & 0 & 0 & \dots \\ & & & & & & & & & & & & & \dots & \dots & \dots \\ & & & & & & & & & & & & & & 1 & 0 \\ & & & & & & & & & & & & & & & 0 \end{bmatrix} \begin{matrix} \text{Row:} \\ 1 \\ 2 \\ 3 \\ 4 \\ \text{Repeat} \\ \text{Repeat} \\ \dots \\ \text{Fourth}-1 \\ \text{Fourth} \\ \text{Fourth}+1 \\ \text{Repeat} \\ \text{Repeat} \\ \dots \\ \text{Half}-1 \\ \text{Half} \end{matrix}$$

$$\text{Dem}^{1/2} = [-1 \quad -1 \quad 1 \quad 0 \quad 0 \quad 0 \quad \dots \quad 0 \quad 0 \quad 2]$$
$$\text{Col} \quad : 1 \quad 2 \quad 3 \quad 4 \quad 5 \quad 6 \quad \dots \quad \text{Half}-2 \quad \text{Half}-1 \quad \text{Half} \qquad (33)$$

Because the new equations were developed from the algorithms, numerical calculation, instead of analytical demonstrations of trigonometric relations, is necessary to check them. It is believed that a large number of numerical tests can validate or verify these new equations, or at least reduce the chance of these equations being wrong or false to a minimum. The goal here is to verify that the new equations really calculate the tangent of the phase $\tan(\phi)$. For that, real figures are attributed to random I_m, which ranges from 0 to 128, which are assigned at random to real values, I_a that ranges from 0 to 127, and the cosine of -1 varies by 1 to the values of luminous intensity I_k will be between 0 and 255, which is the range of pixel values obtained in monochrome digital photos. It is interesting to note that the digital images and values are intact here to further enlarge the test in which they are made real. They are also assigned values to real random ϕ; which varies from $-\pi$ to π, tracking common algorithms used on the main unwrapped. Real values are assigned, and the random δ ranges from -10π to 10π, a very wide range of possible values of step phase. The values of I_k (luminous intensity of the image) are calculated with k ranging from 1 to N. The new equations with the values of I_k are applied, giving a $\tan(\phi)$ that must be compared to the value of phase randomly assigned (ϕ'). This comparison is the accuracy through a very small value because the number of rounding errors that can occur in the calculations (say, precision $|\phi' - \phi| \leq 10^{-6}$). This was done thousands of times (at least 10,000 times) for each equation for phase calculation. It generated and made up of at least 99.9% of the time with an accuracy of 10^{-6}. Thus, it was believed that the chances for the equations to be wrong or false have become minimal or remote.

8 Before Unwrapping, Change $\phi \in [0, \pi/2]$ to $\phi^* \in [-\pi, \pi]$

Because of the character of the evaluation equations, only phase values $\phi \in [0, \pi/2]$ were calculated. For unequivocal determination of the wrapped phase values ϕ, it was necessary to test four values ϕ, $-\phi$, $\phi - \pi$, and $-\phi + \pi$ using values of I_k and small systems. With this, the value $\phi^* \in [-\pi, \pi]$ was obtained.[3–6] In the case $N=5$, with I_1, I_2, I_3, I_4, and I_5, δ was found in the first equation and the values ϕ, $-\phi$, $\phi - \pi$, and $-\phi + \pi$ were attributed to ϕ^* to test the

other equation, and I_a was found using a second equation. As an example, for each (x,y), it was tested for the four values ϕ, $-\phi$, $\phi-\pi$, and $-\phi+\pi$ in (addition and subtraction of first, last, and middle frames, the I_k)

$$\text{even} \quad N=4\begin{cases}\cos(\delta/2)=\pm\left(\dfrac{I_1-I_4}{4(I_2-I_3)}\right)^{1/2}\\ I_1-I_4=2I_a\sin(\phi^*)\sin(3\delta/2)\\ I_2-I_3=2I_a\sin(\phi^*)\sin(\delta/2)\\ (I_1+I_4)-(I_2+I_3)=2I_a\cos(\phi^*)[\cos(3\delta/2)-\cos(\delta/2)]\\ I_1-I_3=I_a[\cos(\phi^*-3\delta/2)-\cos(\phi^*+\delta/2)]\end{cases}, \tag{34}$$

$$\text{odd} \quad N=5\begin{cases}\cos(\delta)=\dfrac{I_1-I_5}{2(I_2-I_4)}\\ I_1-I_5=2I_a\sin(\phi^*)\sin(2\,.\,\delta)\\ I_2-I_4=2I_a\sin(\phi^*)\sin(\delta)\\ I_1+I_5-2\,.\,I_3=2I_a\cos(\phi^*)[\cos(2\,.\,\delta)-1]\\ I_2+I_4-2\,.\,I_3=2I_a\cos(\phi^*)[\cos(\delta)-1]\end{cases}. \tag{35}$$

In a different approach, for unambiguous determination of the wrapped phase values, it is necessary to test four values ϕ, $-\phi$, $\phi-\pi$ and $-\phi+\pi$ using values of I_k and to solve small nonlinear systems (Newton–Raphson methods). For each angle ϕ, $-\phi$, $\phi-\pi$, and $-\phi+\pi$, we solve the nonlinear system by Newton–Raphson in Eq. (36), getting the values of I_m, I_a, and δ,

$$\begin{cases}I_1-\left\{I_m+I_a\cos\left[\phi^*+\left(\dfrac{2.1-N-1}{2}\right)\delta\right]\right\}=0\\ I_2-\left\{I_m+I_a\cos\left[\phi^*+\left(\dfrac{2.2-N-1}{2}\right)\delta\right]\right\}=0\\ I_3-\left\{I_m+I_a\cos\left[\phi^*+\left(\dfrac{2.3-N-1}{2}\right)\delta\right]\right\}=0.\end{cases} \tag{36}$$

With the values of I_m, I_a, and δ, we test Eq. (37) and find the correct angle $\phi^*\in[-\pi,\pi]$.

$$\begin{cases}I_4-\left\{I_m+I_a\cos\left[\phi^*+\left(\dfrac{2.4-N-1}{2}\right)\delta\right]\right\}=0\\ \cdots\\ I_N-\left\{I_m+I_a\cos\left[\phi^*+\left(\dfrac{2N-N-1}{2}\right)\delta\right]\right\}=0.\end{cases} \tag{37}$$

9 Testing and Analysis of Error

The phase ϕ^* obtained from the phase-shifting algorithm above is a wrapped phase, which varies from $-\pi/2$ to $\pi/2$. The relationship between the wrapped phase and the unwrapped phase may thus be stated as follows:

$$\Psi(x,y)=\phi^*(x,y)+2\pi j(x,y), \tag{38}$$

where j is an integer number, ϕ^* is a wrapped phase, and ψ is an unwrapped phase.

The next step is to unwrap the wrapped-phase map. When unwrapping, several of the phase values should be shifted by an integer multiple of 2π. Unwrapping is thus adding or subtracting 2π offsets at each discontinuity encountered in phase data. The unwrapping procedure consists of finding the correct field number for each phase measurement.[10–13]

The modulation phase ψ obtained by unwrapping physically represents the fractional fringe order numbers in the Moiré images. The shape can be determined by applying the out-of-plane equation for shadow Moiré

$$Z(x,y)=\frac{p\left(\dfrac{\Psi(x,y)}{2\pi}\right)}{(\tan\alpha+\tan\beta)}, \tag{39}$$

where $Z(x,y)$=elevation difference between two points located at body surface to be analyzed, p=frame period, α=light angle, and β=observation angle.

The experiments are carried out using a square wave grating with a 1-mm frame grid period; the light source is common white of 300 W without using plane waves; light angle (α) and observation angle (β) are 45 deg; the object surface is white and smooth; and the resolution of photo is one mega pixel. The phase stepping is made by displacing the grid in the horizontal direction in fractions of millimeters (Fig. 5).

To test the new equations for phase calculation, they were used with the technique of shadow Moiré[13] for an object with known dimensions and to evaluate the error median by Eq. (40). This process was started with four images, repeated with five, then six, and so on. The idea was to show that with an increasing number of images the average error tends to decrease. Figure 6 shows this procedure.

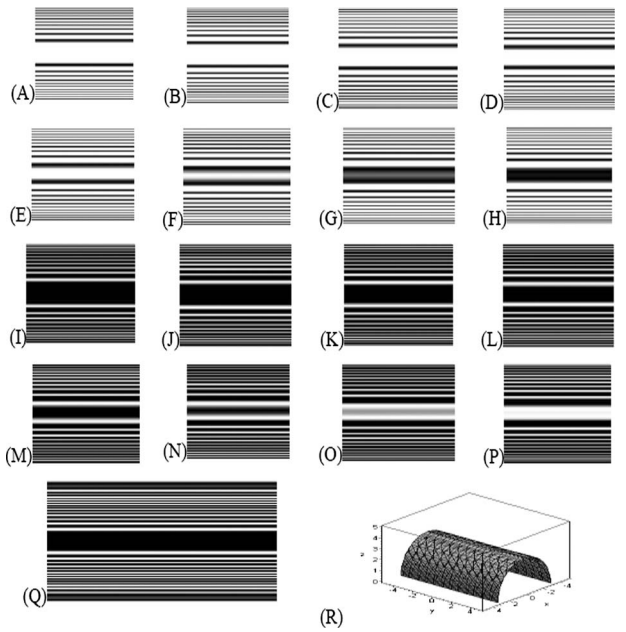

Fig. 6 One set of photos of 1 Mb (with low-pass filter and Gaussian filter). Original shadow moiré images. 16-frame phase-shifting algorithm (A–P). Wrapped phase (Q). Result in three dimensions (R). (Semicylinder of a motor with diameter 6 cm, length 12 cm, and with frame period of grid 1 mm).

$$\text{Error Median } (E) = \frac{1}{M}\sum_{i=1}^{M} |Z_i^e - Z_i|, \tag{40}$$

where M is the number of pixels of the image, Z_i^e is the exact value of the size of the object being measured, and Z_i is value measured by the new equation.

To compare the new equations for calculating the phase, 21 sets of 16 photos each were selected. Each set was computed using the average error of 4 to 16 images and using equations to evaluate the number of images. An average of errors was estimated, then 21 sets were evaluated using 4 to 16 images in each set $(\mu_4, \mu_5, \mu_6, \ldots, \mu_{16})$. The hypothesis of testing on the difference in the means $\mu_A - \mu_B$ of two normal populations is being considered at the moment. A more powerful experimental procedure is to collect the data in pairs—that is, to make two hardness readings on each specimen, one with each tip. The test procedure would then consist of analyzing the differences between the hardness readings on each specimen. If there is no difference between tips, then the mean of the differences should be zero. This test procedure is called the paired t-test.[14] Specifically, testing $H_0: \mu_A - \mu_B = 0$ against $H_1: \mu_A - \mu_B \neq 0$. Test statistics is $t_0 = D/(S_D/\sqrt{21})$, where D is the sample average of the differences and S_D is the sample standard deviation of these differences. The rejection region is $t_0 > t_{\alpha/2,20}$ or $t_0 < -t_{\alpha/2,20}$. The data are shown in Table 2.

On performing the statistical test ($H_0: \mu_A - \mu_B = 0$ against

Table 2 Error median error in μm versus number of frames (N) for semicylinder with diameter of 6 cm and length of 12 cm (frame period of grid with 1 mm). It used 21 different sets of 16 images of shadow Moiré (Fig. 6).

Error median (μm)	Sets of images																				
Number of images	1	2	3	4	5	6	7	8	9	10	11	12	13	14	15	16	17	18	19	20	21
4	125	127	125	128	129	128	126	125	128	127	127	127	129	127	127	127	127	127	126	126	127
5	121	122	122	123	123	124	123	123	124	121	122	121	123	124	122	124	125	122	121	123	121
6	118	118	118	119	120	120	119	120	120	120	121	119	119	117	117	118	121	118	119	121	119
7	113	113	116	117	115	113	116	113	115	115	113	116	115	113	115	116	116	113	113	116	114
8	109	110	111	110	110	111	111	109	112	110	111	112	109	112	110	111	111	112	112	110	110
9	107	105	107	106	106	107	106	107	105	107	104	107	106	108	104	107	104	104	105	105	105
10	103	104	103	102	104	103	102	101	102	102	104	103	103	102	100	101	104	100	103	101	100
11	99	100	98	99	98	100	97	96	98	98	100	100	98	98	99	99	99	99	99	96	100
12	94	94	95	93	92	93	95	95	95	96	95	95	95	92	93	93	92	93	92	95	92
13	89	89	91	88	90	89	90	88	92	91	90	88	88	88	91	88	88	89	90	89	89
14	84	84	87	87	85	87	85	86	86	87	84	87	86	87	84	84	85	87	85	84	87
15	82	81	83	84	81	81	85	83	83	85	82	83	85	81	83	82	85	85	84	85	83
16	79	81	78	77	78	78	78	81	80	78	79	79	78	80	80	80	78	78	77	81	78

Table 3 Testing hypotheses about the difference between two means with paired t-test, $H_0: \mu_A - \mu_B = 0$ against $H_1: \mu_A - \mu_B \neq 0$. The P value is the smallest level of significance that would lead to rejection of the null hypothesis H_0 with the given data.

P-value	Number of images											
Number of image	$N=4$ (%)	$N=5$ (%)	$N=6$ (%)	$N=7$ (%)	$N=8$ (%)	$N=9$ (%)	$N=10$ (%)	$N=11$ (%)	$N=12$ (%)	$N=13$ (%)	$N=14$ (%)	$N=15$ (%)
$N=4$												
$N=5$	0											
$N=6$	0	0										
$N=7$	0	0	0									
$N=8$	0	0	0	0								
$N=9$	0	0	0	0	0							
$N=10$	0	0	0	0	0	0						
$N=11$	0	0	0	0	0	0	0					
$N=12$	0	0	0	0	0	0	0	0				
$N=13$	0	0	0	0	0	0	0	0	0			
$N=14$	0	0	0	0	0	0	0	0	0	0		
$N=15$	0	0	0	0	0	0	0	0	0	0	0	
$N=16$	0	0	0	0	0	0	0	0	0	0	0	0

$H_1: \mu_A - \mu_B \neq 0$) it was noted that one cannot reject the zero hypothesis when using different equations with the same number of images. Also, the null hypothesis can be rejected when using different equations with a different number of images with a level of significance ($\alpha=0.05$). It was concluded that the equations for phase calculation with a greater number of images are more accurate than those with a smaller number of images. The tests are shown in Table 3.

With the generalization of the Carré equation, it was possible to develop a shadow Moiré system that moves the grid with constant speed while a camera takes many pictures at equal intervals of times, like a film. With that obtained, measures are more precise and there are less uncertainties.

10 Conclusion

The new equations are shown to be capable of processing the optical signal of Moiré images. The results show that the new equations are very precise, easy to use, and have a small cost. On the basis of the performed error analysis, it can be concluded that the new equations are very good phase calculation algorithms. These equations also seem to be a very accurate and stable phase-shifting algorithms with the unknown phase step for a wide range of phase-step values. The metric analysis of the considered system demonstrated that its uncertainties of measurement depend on the frame period of the grid, of the resolution of photos in pixels, and of the number of frames. In theory, if there are many frames, then the measurement errors become very small. The measurement results obtained by the optical system demonstrate its industrial and engineering applications.

Acknowledgment

The authors appreciate the generous support of the Pontificia Universidade Catolica de Minas Gerais—PUCMINAS, as well as of the Conselho Nacional de Desenvolvimento Cientifico e Tecnologico–CNPq, National Counsel of Technological and Scientific Development.

References

1. H. Schreiber and J. H. Bruning, "Phase shifting interferometry," in *Optical Shop Testing*, D. Malacara, Ed., p. 547, Wiley, Hoboken, NJ (2007).
2. D. Malacara, M. Serv'in, and Z. Malacara, *Interferogram Analysis for Optical Testing*, p. 414, Taylor & Francis, New York (2005).
3. K. Creath, "Phase-measurement interferometry techniques," in *Progress in Optics*, Vol. **XXVI**, E. Wolf, Ed., p. 349, Elsevier Science Publishers, Amsterdam (1988).
4. J. Novak, "Five-step phase-shifting algorithms with unknown values of phase shift," *Optik (Jena)* **114**(2), 63–68 (2003).
5. J. Novak, P. Novak, and A. Miks, "Multi-step phase-shifting algorithms insensitive to linear phase shift errors," *Opt. Commun.* **281**(21), 5302–5309 (2008).
6. P. S. Huang and H. Guo, "Phase-shifting shadow moiré using the Carré algorithm," *Proc. SPIE* **7066**, 70660B (2008).
7. D. Malacara Ed., *Optical Shop Testing*, Wiley, Hoboken, NJ (1992).
8. R. R. Cordero, J. Molimard, A. Martinez, and F. Labbe, "Uncertainty analysis of temporal phase-stepping algorithms for interferometry," *Opt. Commun.* **275**(1), 144–155 (2007).
9. F. S. Hillier and G. J. Lieberman, *Introduction to Operations Research*, 8th ed. McGraw-Hill, New York (2005).
10. D. C. Ghiglia and M. D. Pritt, *Two-Dimensional Phase Unwrapping: Theory, Algorithms and Software*, Wiley, Hoboken, NJ (1998).
11. J. M. Huntley, "Noise-immune phase unwrapping algorithm," *Appl. Opt.* **28**, 3268–3270 (1989).

12. E. Zappa and G. Busca, "Comparison of eight unwrapping algorithms applied to Fourier-transform profilometry," *Opt. Lasers Eng.* **46**(2), 106–116 (Feb. 2008).
13. C. Han and B. Han, "Error analysis of the phase-shifting technique when applied to shadow moiré," *Appl. Opt.* **45**, 1124–1133 (2006).
14. M. F. Triola, *Elementary Statistics*, 10th ed., Addison Wesley, Boston (2007).

Pedro Americo Almeida Magalhães, Jr., received his bachelor's degree in electrical engineering from the Universidade Federal de Minas Gerais and his bachelor's degree in computer science from Pontificia Universidade Catolica de Minas Gerais (PUC-MG), Belo Horizonte, Brazil, in 1989. He received a specialist diploma in material engineering from Fundacao Educacional Minas Gerais in 1995, as well as a master's degree in electrical engineering and a doctorate in mechanical engineering in 2001 and 2009, respectively, both from PUC-MG. He is currently a numeric methods teacher at the Mathematics Department of PUC-MG, Brazil.

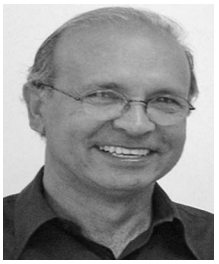

Perrin Smith Neto completed his undergraduate degree in mechanical engineering at the Universidade Federal de Minas Gerais in 1969. He performed postgraduate work in photoelastic analysis at University of Stuttgart from 1977 to 1980 and in microelectronics in sensors and actuators at Fachhoschule Akademie Esslingen, Germany in 1979. He received his master's degree in engineering from the University of Sao Paulo in 1976 and his doctorate in engineering from the University of Sao Paulo in 1980, and he performed postdoctoral studies at University of British Columbia, Vancouver, Canada, in 1988. He was a professor at the Universidade Federal de Uberlandia, Brazil, from 1970 to 1996. He has been a full professor in the Mechanical Engineering Department at Pontificia Universidade Catolica de Minas Gerais since 1996.

Cristina Almeida Magalhães received her bachelor's degree in civil engineering from the Universidade Federal de Minas Gerais in 2005, and her master's degree in computer science from Pontificia Universidade Catolica de Minas Gerais in 2008. She is currently pursuing a doctorate in mechanical engineering at Pontificia Universidade Catolica de Minas Gerais, Brazil.

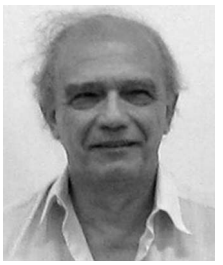

Clovis Sperb de Barcellos completed his undergraduate degree in mechanical engineering at the Universidade Federal do Rio Grande do Sul in 1967, his master's degree in mechanical engineering at Pontificia Universidade Catolica do Rio de Janeiro in 1970, and his doctorate in engineering mechanics at the University of Minnesota in 1977. He is currently a retired professor of the Universidade Federal de Santa Catarina, Universidade Presbiteriana Mackenzie, Ministerio da Educação, and Conselho Nacional de Desenvolvimento Cientifico e Tecnologico, Santa Catarina, Brazil.